

Investigating the Kinetic Effects on Current Gradient-Driven Instabilities of Electron Current Layers via Particle-in-Cell Simulations

Sushmita Mishra,¹ Gurudatt Gaur,^{2,3} and Bhavesh G. Patel⁴

¹*Institute of Advanced Research, Koba Institutional Area, Gandhinagar 382 426, India*

²*St. Xavier's College (Autonomous), Navrangpura, Ahmedabad 380 009, India*

³*Kshama Ahmedabad Academy of Sciences, Motera, Ahmedabad 380 005, India*

⁴*Institute for Plasma Research, Bhat, Gandhinagar 382 428, India*

(*Electronic mail: gurudatt.gaur@sxca.edu.in)

(*Electronic mail: mishra.sushmita0@gmail.com)

(Dated: 27 August 2024)

Electron current layers form in various natural and laboratory plasmas and are susceptible to several instabilities. Tearing, driven by current gradients, stands out as a prominent instability in these layers and is considered a potential mechanism for magnetic reconnection in collisionless regimes. Electron inertia serves as a non-ideal factor causing magnetic field lines to break and subsequently reconnect. Another mode driven by current gradients, known as the surface-preserving mode, maintains magnetic field topology. We investigated the kinetic effects on these modes in the presence of finite electron temperatures using two-dimensional particle-in-cell simulations (implemented with the OSIRIS codebase). Temperature stabilizes the tearing mode to a large extent, except at low temperatures, due to increased electron Larmor radius and subsequent magnetic field diffusion. Introducing uniform guide fields revealed that growth rates decrease at higher temperatures due to reduced plasma beta. Conversely, for the surface-preserving mode, growth rates increase with temperature, likely due to enhanced electron flow velocities. Mixed modes, where both tearing and surface-preserving modes coexist, exhibit asymmetric structures characteristic of asymmetric magnetic reconnection. Finally, we propose future research directions building upon our findings.

I. INTRODUCTION:

Plasma is a state of matter in which electrons and ions move freely, exhibiting collective behavior under the influence of electric and magnetic fields produced either by their own motion or by external sources. Studying plasma properties is essential for understanding various natural phenomena and for advancing technological applications. This research often involves measurements on natural plasmas and sophisticated laboratory experiments to study plasma behavior under different conditions.

Magnetic fields significantly influence plasma dynamics, leading to rich and complex behaviors. They affect the motion of charged particles, which in turn modify the magnetic fields due to the frozen-in condition arising from the high electrical conductivity of plasmas. One key phenomenon where the magnetic field is altered by plasma particles is magnetic reconnection (MR). In MR, plasma pushes two oppositely directed magnetic field lines towards each other, changing the topology of the magnetic field lines.¹ MR is observed in various natural settings, including the solar system. It plays a crucial role in solar flares, coronal mass ejections, the Earth's magnetosphere, and astrophysical jets. MR is also believed to occur during star formation. Additionally, MR is observed in several fusion plasma devices, such as Tokamak, Reverse Field Pinch, and Spheromak^{2,3}. Numerous laboratory plasma devices have been created to understand the mechanisms behind MR.⁴⁻⁶

Significant efforts have been made to propose theoretical models explaining MR at different time and length scales in various plasma conditions. The resistive MHD (magnetohydrodynamics) models, such as the Sweet-Parker model and

the Petschek model, describe MR occurring in a long, narrow current sheet with a reconnection rate limited by plasma resistivity. The Sweet-Parker model^{7,8} predicts a slow reconnection rate, insufficient to explain the fast reconnection events observed in nature, whereas the Petschek model⁹ suggests a faster reconnection process but is less applicable to collisionless plasmas. Space and astrophysics plasmas, where fast reconnection occurs, are known to be collisionless. In a collisionless plasma, where the mean free path of particles is much larger than the system size, the reconnection dynamics are predominantly governed by the electromagnetic forces rather than collisional interactions.

Various models have been proposed to understand fast reconnection in collisionless plasmas, addressing different aspects and scales of the process, both fluid and kinetic. While the MHD model is valuable for understanding large-scale plasma behavior, it is insufficient for describing the detailed physics of collisionless MR. For collisionless plasmas, models which include electron scale dynamics such as EMHD (electron magnetohydrodynamics)¹⁰, Hall MHD, and two-fluid MHD,¹¹⁻¹⁴ or the models that include kinetic effects, such as hybrid¹⁵ and full kinetic (PIC: particle-in-cell) models,^{16,17} are necessary to accurately capture the complex dynamics and fast reconnection rates observed in these environments. These models incorporate the Hall term and electron inertia, leading to faster reconnection rates and more complex magnetic island structures than single-fluid MHD models can provide.

While the fluid picture is suitable for most of the natural and laboratory plasmas and provides a relatively simple description of plasma behavior, it breaks down in situations where kinetic effects, high-frequency phenomena, strong magnetic

fields, turbulence, collisionless dynamics, and microscopic processes play a dominant role. Particle-in-cell (PIC) simulations provide a more detailed approach by modeling individual particles and their interactions, capturing the full kinetic behavior of plasmas.¹⁸ PIC methods are particularly suited for investigating the microscale processes such as the formation of electron and ion diffusion regions, the development of current sheets, and the dynamics of magnetic islands. The electron diffusion region (EDR) is critical for collisionless reconnection, where electrons decouple from magnetic field lines. PIC simulations have revealed complex structures within the EDR, including crescent-shaped electron velocity distributions and the formation of electrostatic fields that facilitate reconnection.¹⁹ In the ion diffusion region (IDR), PIC simulations by Hesse et al., have highlighted the role of ion-scale structures and kinetic Alfvén waves in the reconnection process.²⁰ Drake et al., via PIC simulations studies have demonstrated that guide fields can stabilize the current sheet, alter the structure of magnetic islands, and affect particle acceleration mechanisms.²¹

A specific manifestation of magnetic reconnection (MR) is the tearing instability, which represents a dynamic approach to studying MR. Unlike the steady state approaches exemplified by the Sweet-Parker and Petschek models, the tearing instability involves the formation of a chain of magnetic islands and reconnection layers. This process leads to a reconfiguration of the magnetic topology. The tearing mode evolves according to parameters such as the width of the current sheet (ϵ) and the length scales characteristic of kinetic effects. These include the electron inertial skin depth (d_e), the ion inertial skin depth (d_i), and the Larmor radius of electrons or ions (r_L).¹⁴ Tearing instability of thin current layers, of thickness smaller than the ion skin depth, has been studied by many researchers in the context of 2D and 3D EMHD.

Gaur and Kaw, in the context of 2D EMHD, studied the susceptibility of electron current configurations to tearing and surface preserving instabilities when the equilibrium length scales are less than the ion skin depth.²² Although both modes are driven due to equilibrium current-gradient, their evaluation is completely different. While the tearing mode leads to the formation of magnetic islands, the surface-preserving mode, on the other hand, preserves the surface of magnetic flux. Moreover, the tearing mode is a non-local mode while the surface-preserving mode is a local mode (unstable to the perturbations having wavelengths smaller than the equilibrium length scale). In this paper, we aim to study the kinetic effects of these two modes, such as the effect of temperature, and the interplay between temperature and the guide field. Fluid descriptions like EMHD break down at the kinetic scales, for instance, for hot plasmas or when the length scales are smaller than the gyroradius. Therefore, we have carried out particle-in-cell simulations to understand the linear and nonlinear stages of the two modes in the presence of kinetic effects.

The tearing and surface-preserving mode together have been previously studied by Lukin²³, Gaur and Kaw²² and Jain et al.,^{24,25} within the EMHD framework. Our research advances this work by exploring the kinetic effects in the pres-

ence of temperature using 2D Particle-in-Cell (PIC) simulations. To our knowledge, no prior work has been done on these lines.

The paper is organized as follows. In Section II, we discuss the basics of the particle-in-cell scheme along with the simulation setup we have used. In Section III, we present the results and discussions on various simulation runs we have conducted. We also present a comparison of our work with the existing studies and highlight the novelty of our work. In Section IV, we provide the conclusion.

II. PARTICLE-IN-CELL (PIC) METHOD AND SIMULATION SETUP

Particle simulation model can be classified into three principal types: the particle-particle (PP) model, the particle-mesh (PM) model, and the particle-particle-particle-mesh (PPPM or P3M) model.²⁶ The PP model utilizes the action-at-a-distance approach of the force law, the PM model implements the force as a field quantity (approximating it on a mesh), and the P3M model incorporates characteristics of both the PP and PM models.

The Particle-in-Cell (PIC) method is based on the PM model. In PIC simulations, the plasma is represented by a large number of superparticles, each representing a cluster of real particles, typically electrons and ions. These superparticles move through a computational grid (mesh) where the electromagnetic fields are calculated. The position and velocity of each particle are given as initial conditions, which determine the continuous distribution of the particles' position and velocity in space.

The PIC algorithm involves a self-consistent cycle: assigning charge to the mesh, solving Maxwell's equations and computing the fields from the mesh-defined potential, and updating the particle velocity and position based on the fields. Fig. 1 shows the algorithm for the PIC technique, which includes the Boris scheme for pushing particles and a finite difference solver for the field calculations. There are various PIC codes available for plasma simulations; some of the widely used are VPIC (Vector Particle-In-Cell), iPIC3D, P3D, GEM (Geospace Environment Model) and OSIRIS.

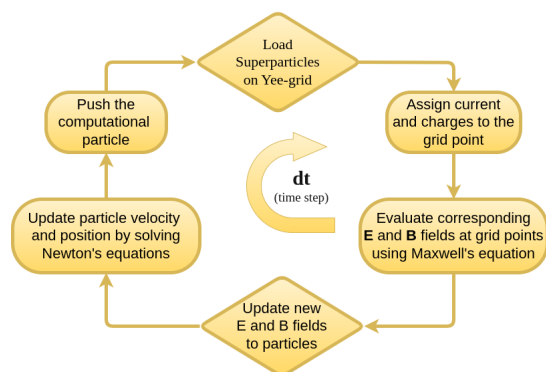


FIG. 1. PIC Algorithm

OSIRIS is a state-of-the-art PIC simulation code that is fully relativistic, massively parallel and fully object-oriented. Written in Fortran-90, it is designed for high-performance computing with multi-dimensional capabilities²⁷. OSIRIS simulates the behavior of plasmas by solving the Vlasov-Maxwell equations using the PIC method and is optimized for large-scale parallel supercomputers, utilizing the Message Passing Interface (MPI) for communication between processors²⁸.

Widely used in plasma physics research, OSIRIS features comprehensive physics models, including electromagnetic fields, relativistic particle dynamics, collisions, and radiation mechanisms. It excels in modeling complex plasma interactions, such as laser-plasma interactions for inertial confinement fusion²⁹ and particle acceleration in astrophysical phenomena like magnetic reconnection, gamma-ray bursts, and relativistic jets³⁰.

We have utilized the OSIRIS 4.0 framework³¹ to model the 2D tearing and surface preserving instabilities. In our simulations, the normalized units are defined as follows: length is normalized by electron skin depth c/ω_{pe} , time is normalized by ω_{pe}^{-1} , and magnetic field by the quantity $\frac{m_e c^2}{e(c/\omega_{pe})}$. Where c is the speed of light, ω_{pe} is the electron plasma frequency, and m_e is the electron mass.

We have initialized our simulations for a thin current sheet equilibrium having width of the magnitude ε and z is the symmetry direction i.e., $(\frac{\partial}{\partial z}) = 0$. Ions are at rest (i.e., $v_i = 0$). Equilibrium magnetic field is expressed as follows:

$$\mathbf{B}_{eq} = \hat{y}B_0(x) = B_{00}\{\text{sech}(x/\varepsilon)\tanh(x/\varepsilon)\} + C_0, \quad (1)$$

Corresponding equilibrium velocity is written as,

$$\begin{aligned} \mathbf{v}_{eq} (= -\nabla \times \mathbf{B}_{eq}) &= \hat{z}v_0(x) \\ &= \frac{B_{00} \sinh^2(x/\varepsilon)}{\varepsilon \cosh^3(x/\varepsilon)} \end{aligned} \quad (2)$$

Where, ε is shear width, B_{00} is the amplitude of the magnetic field, C_0 is a uniform magnetic field added externally in the direction of field.

In all our simulation runs, we have chosen $B_{00} = 0.1$ and $\varepsilon = 1$. A 2D rectangular simulation box with dimensions $L_x = 8(c/\omega_{pe})$ and $L_y = 3(c/\omega_{pe})$ has been chosen. The spatial resolution corresponds to a grid size of $\Delta x = 2L_x/512$ and $\Delta y = 2L_y/256$. A uniform plasma number density $n_0 = 10^{18} \text{cm}^{-3}$ has been chosen. We allow the equilibrium to evolve against the numerical perturbations. We have taken a periodic boundary conditions for both fields and particles because the equilibrium profile chosen is such that it ceases at both the boundaries. The equilibrium magnetic field and the corresponding equilibrium velocity profiles are shown in Fig. 2. Three different magnetic field profiles corresponds to three different values of C_0 viz., 0, 0.025, 0.06.

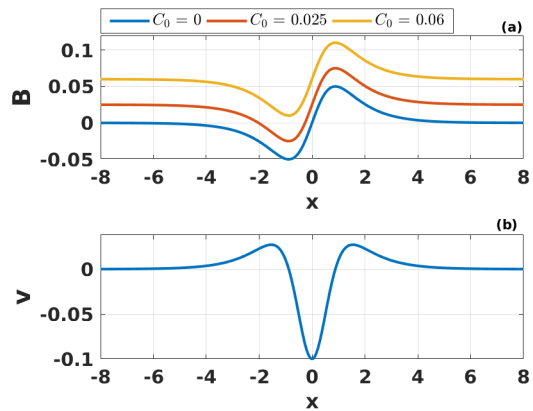


FIG. 2. (a) Equilibrium \mathbf{B} and (b) corresponding equilibrium \mathbf{v} profiles.

III. RESULTS AND DISCUSSION

In this section we present and discuss the results from various simulation runs obtained by varying the C_0 (a uniform magnetic field applied along the equilibrium magnetic field) and T (temperature).

A. $C_0 = 0$: Only Tearing Mode Case

We first choose $T = 0$. This is the typical tearing instability case which has been studied by various authors in past using fluid as well as PIC simulations. We have (re)produced this run to validate our simulation setup. In Fig. 3 we have plotted the evolution of perturbation energy. The rate at which the perturbation energy grows matches well with the growth rate obtained from the linear instability calculations²². In Fig. 4, the contours in the background depict the structure of the out-of-plane magnetic field. The magnetic field lines, superimposed on these contours, are straight, initially. However, as the tearing instability progresses, these field lines begin to bend, eventually forming an island structure. Concurrently, the out-of-plane magnetic field develops a distinctive quadrupolar pattern. These features are characteristic indicators of the tearing instability.

Having validated the simulation setup, we now proceed to study the effect of temperature on tearing instability. We conduct simulation runs for the following temperature values: ($T = 5, 10, 20, 50, 100, 200, 500, 1000$) electron volts. Upon increasing the temperature, while the characteristic features of the instability (such as the formation of islands and quadrupoles) remain more or less the same, we observe a variation in the growth rate with temperature. Fig. 5 illustrates the variation in the growth rate as temperature increases. The growth rate initially increases with temperature and then starts decreasing monotonically. This behavior can be understood as follows.

Initially, when the temperature increases (say, up to 10 eV), the kinetic energy of the electrons increases. This makes

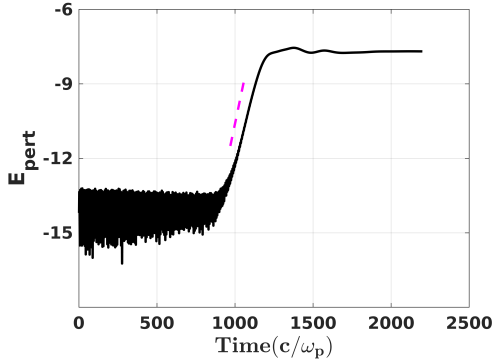


FIG. 3. The rate of evolution of perturbed energy obtained from the PIC simulation matches with the growth rate calculated from linear analysis under the EMHD model (dashed line) for the tearing mode at $T = 0$ eV.

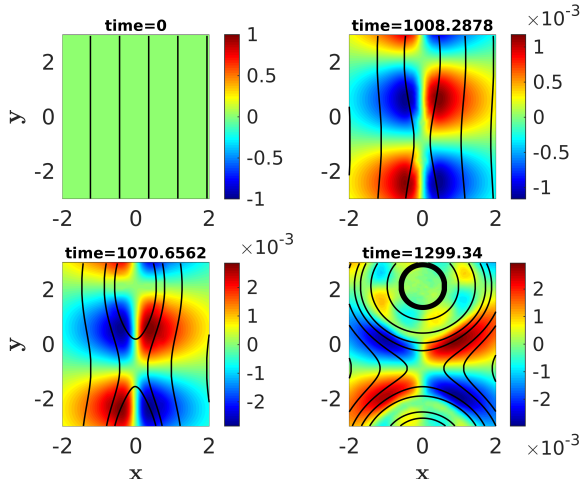


FIG. 4. Shaded isocontours of out-of-plane magnetic field with superimposed streamlines (solid lines) over various times for $C_0 = 0$ and $T = 0$ eV case.

the tearing instability more favorable, as the electrons move faster in the tearing instability plane compared to the case with $T = 0$. Consequently, the instability growth rate increases marginally. If the temperature further increases (beyond 10 eV), electron larmor radius (r_L) increases significantly, which is given as $r_L = v_{th}/\omega_{ce}$, where $v_{th} = \sqrt{p_e/(nm)}$ and $\omega_{ce} = eB/(m_e c)$ are the thermal velocity and plasma cyclotron frequency respectively. In other words, kinetic pressure starts dominating the the magnetic pressure i.e., the plasma beta (β) value increases, where $\beta = (n_e k_B T / (B^2 / 2\mu_0))$. This increases the diffusion of magnetic field (not just near the null-line) which, in turn, reduces the strength of current-gradient (due to weaker magnetic field and hence weaker current). As a result, the growth rate decreases. Eventually, at $T \geq 1keV$, the instability completely suppresses.

To reinforce our argument on the role of larmor radius in tearing growth rate against temperature, we add a uniform guide field³² (in the direction perpendicular to the plane of tearing mode). Addition of guide field increases the magnetic

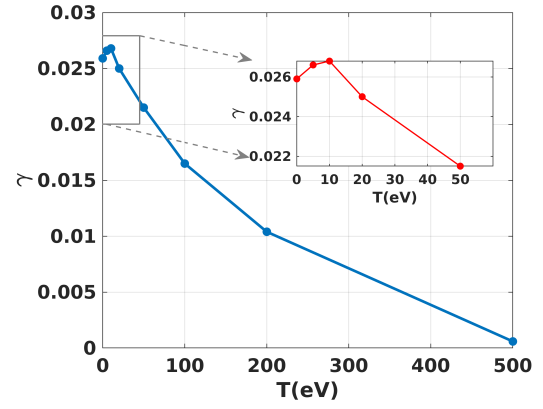


FIG. 5. The variation in growth rate calculated for the evolution of perturbed energy for $C_0 = 0$ case with temperatures (T) in eV . The inset figure highlights growth rate changes for $T = 0, 5, 10, 20$ and 50 eV

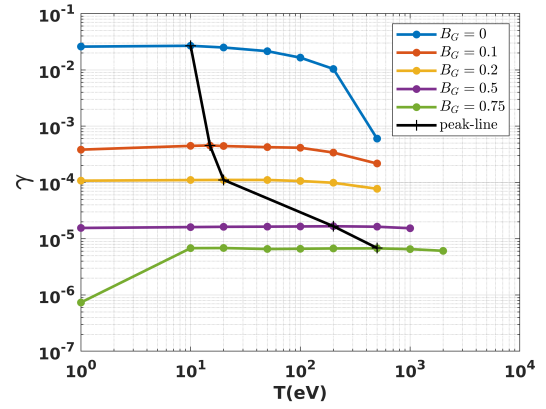


FIG. 6. Growth rate of perturbed energy evolution for $C_0 = 0$ with varying guide field values and temperatures. The black line denotes the peak value for each growth rate curve at different guide field values.

pressure (energy) of the system. Owing to which, the decrease in the growth rate now start dropping at a higher temperature. Fig. 6 shows that as the guide field increases, the peak in the growth rate shift towards higher temperature.

B. $C_0 = 0.06$: Only Surface Preserving Mode Case

We now add C_0 , a uniform magnetic field along the direction of equilibrium magnetic field. We choose $C_0 = 0.06$, as this would make the condition $B_0 - B_0'' \leq 0$ for the existence of the tearing mode to be violated. Coincidentally, the opposite condition $B_0 - B_0'' > 0$ favors the existence of the surface preserving instability. Hence, only the surface preserving mode will be present in this case²².

Simulation run with $T = 0$ eV, show no formation of quadrupoles or islands, which is unlike the tearing mode scenario. Magnetic field lines in this case do not bend and instead

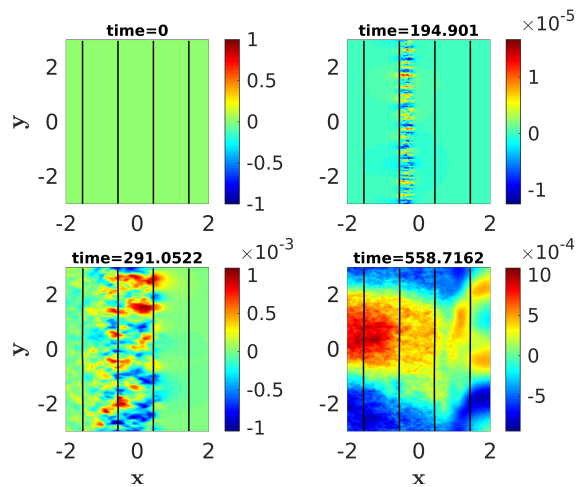


FIG. 7. Shaded isocontours of out-of-plane magnetic field with superimposed streamlines (solid lines) over various times for $C_0 = 0.06$ and $T = 0$ eV case.

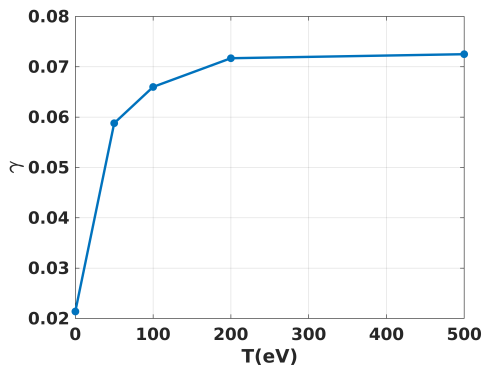


FIG. 8. The variation in growth rate calculated for the evolution of the perturbed energy of $C_0 = 0.06$ case with temperatures (T) in eV.

form a channel-like structure, as depicted in Fig. 7. In order to understand the behaviour of growth rate of surface preserving mode we conduct simulation runs for the following temperature values: ($T = 5, 10, 20, 50, 100, 200, 500$) electron volts. In Fig. 8, we plot the growth rate vs temperature. In this case, the growth rate goes on to increase, unlike the tearing mode case where the growth rate first increases and then start decreasing after a certain temperature. This can be explained as follows. Surface preserving mode, also termed as stationary nontearing inertial scale mode, is driven by the electron flow perturbations along the direction of the current gradient²³. An increase in temperature increases the electron flow velocity which, in turn, makes the instability more favourable.

C. $C_0 = 0.025$: Mixed Modes Case

In this last case, we choose $C_0 = 0.025$. This value of C_0 permits both tearing and surface preserving modes to exist simultaneously. Due to the presence of tearing mode, the ini-

tially straight magnetic field lines evolve and then form an island. However, unlike the only tearing mode case (for $C_0 = 0$), the island formed in this case is asymmetric (see Fig. 9). The asymmetry is also observed in the evolution of out-of-plane magnetic field, the quadrupole formed is asymmetric.

Another interesting observation we made is that the island does not remain at its original location; it moves towards the left, the side with the weaker magnetic field. In Fig. 10, we see that initially the island forms at the null-line, denoted by a vertical line (at $x = -0.2661$), and it is asymmetric. As time progresses, the island shifts leftward. As seen in last subplot, the island has moved away from the vertical null-line. In contrast, in the case of only the tearing mode, a symmetric island forms at the null-line (at $x = 0.0$ in this case) and remains there, as shown in various subplots of Fig. 11. Shaded isocontours of equilibrium current show the formation of mushroom-like patterns. Two jet-like electron flows emerge from the neighboring X-points, which are essentially the outflows from two adjacent reconnection sites. These flows collide at the center of the O-point and then move perpendicularly to impact the closed magnetic surfaces on opposite sides, creating the mushroom-like structures. In the mixed modes case, the two electron flows encounter different strengths of the magnetic field on either side of the null-point. The stronger magnetic field experiences less bending due to higher magnetic tension. The collision of electron flows with magnetic surfaces of unequal strengths results in a net momentum toward the left. This net momentum causes the island and other structures to move in the negative x-direction. The unequal magnetic field strength on the two sides of the null-line is also the reason behind the formation of asymmetric structures. Some of these features have been reported in studies on asymmetric magnetic reconnection, which has recently garnered significant interest.

To understand the role of temperature, we conducted simulation runs for the following temperature values: $T = 5, 10, 20, 50, 100, 200, 500$ electron volts. Figure 12 depicts the change in growth rate with temperature for this case. Similar to the case with only the tearing mode, the growth rate first increases with temperature and then starts decreasing. However, the peak of the curve has shifted to a lower temperature. Specifically, the peak growth rate occurs around 5 eV, compared to 10 eV in the only tearing mode case. The reason for this leftward shift of the peak is not certain at present. It could be due to asymmetry in the magnetic field on two sides of the null-line, the co-existence of the surface-preserving mode, and the effect of temperature on them. A more detailed study is underway to understand this effect.

Comparison with the Existing Studies:

Resistive MHD model can not explain the fast reconnection. Collisionless reconnection is one of the most promising models to explain the same. A vast literature is available on collisionless reconnection where hall term and inertia term become important. But most of these studies include the ion motion as well. Electron scale tearing mode is considered to be

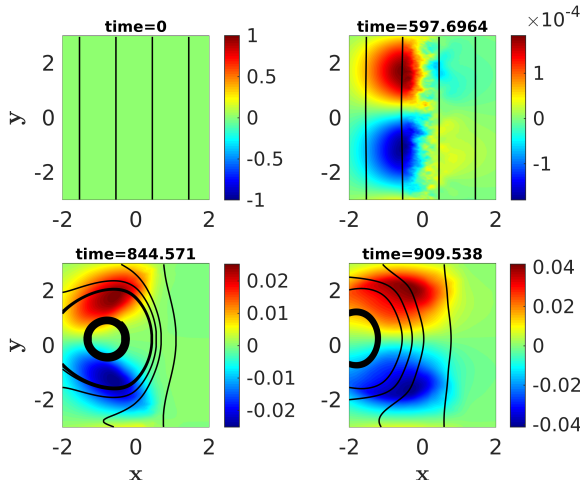


FIG. 9. Shaded isocontours of out-of-plane magnetic field with superimposed streamlines (solid lines) over various times for $C_0 = 0.025$ and $T = 0$ eV case.

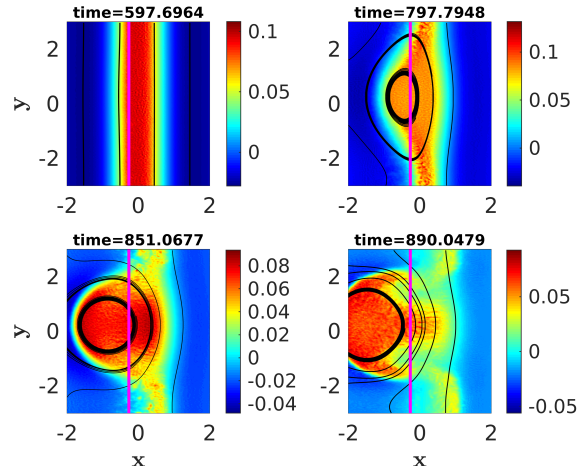


FIG. 10. Shaded isocontours of the current J_z with superimposed streamlines (black lines) over various times for $C_0 = 0.025$ and $T = 0$ eV case.

a prominent mechanism behind the fast reconnection. Studies that focus on the motion of only electrons by assuming the ions to be at rest, like our studies presented in this paper. We compare our results with the previous studies those have considered electrons motion only.

Electron scale tearing instability has been studied using Electron Magnetohydrodynamics (EMHD) model and Particle-In-Cell (PIC) simulations. Cai and Li³³, studied the pressure gradient effects on tearing mode in the presence of guide magnetic field by including the electron pressure tensor, using EMHD model. Our numerical simulations are consistent with their analytical studies which show that when the electron thermal Larmor radius becomes sufficiently large, it can suppress the tearing mode instability. In one of their earlier works, Cai and Li³⁴, had included the compressible effects. However, our PIC simulations do not include the com-

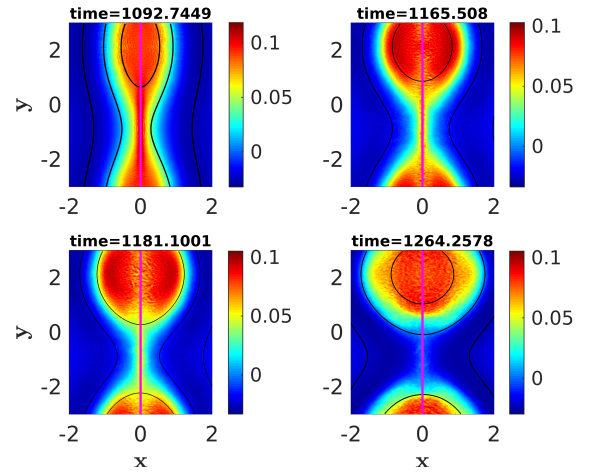


FIG. 11. Shaded isocontours of the current J_z with superimposed streamlines (black lines) over various times for $C_0 = 0$ and $T = 0$ eV case.

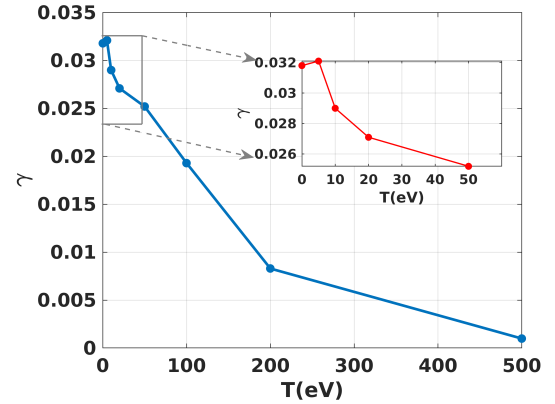


FIG. 12. The variation in growth rate calculated for the evolution of perturbed energy for $C_0 = 0.025$ case with temperatures (T) in eV. The inset figure highlights growth rate changes for $T = 0, 5, 10, 20$ and 50 eV

pressible effects and focus on the kinetic effects and specifically examine how temperature variations influence the tearing mode. Studies by Cai et al., are limited to linear regime only, while our simulations explore the nonlinear regime as well.

Jain & Büchner²⁴ conducted 3D linear studies focusing on tearing and non-tearing modes, examining the dependence of growth rate on the thickness of the electron current sheet, the strength of the guide field, and the wavenumber of the modes. Later, Jain et al.²⁵ performed 3D simulations to study these effects in the nonlinear regime. The key difference in our work is the inclusion of temperature effects, with no perturbations assumed along the equilibrium velocity current.

Guo et al.³⁵ analyzed the density and pressure gradient effects on the tearing mode in the context of 2D EMHD to study the electron diamagnetic drift and Biermann battery effects. In their later studies, Guo et al.³⁶ explores the tearing mode in-

stability within electron-skin-depth-scale current sheets using EMHD model. The study conducts linear simulations of the tearing mode in both Harris sheet and force-free current sheet configurations, revealing that resistive diffusion is negligible at this scale. Additionally, the study examines the impact of a strong magnetic guide field and shear flow, finding that shear flow can suppress the tearing mode in a force-free equilibrium state. Our research, on the other hand, does not consider density and pressure gradients or shear flow, but rather focuses on the interplay between electron temperature and the guide field.

The contour plots for magnetic field, current and other fields observed in our PIC simulations exhibit the same behavior as observed by Sarto et al.³⁷ during the fully nonlinear phase of the EMHD reconnection. We have also observed the secondary Kelvin – Helmholtz instability of the current jets originating from two nearby X points colliding at the O point. However, in the case of mixed mode, we observe that the collision of the two jets results in the net momentum and make the island and other structure move from the position they initially form. No such phenomena was observed in the case of only surface-preserving mode case.

Betar et al.³⁸ conducted a numerical study on the linear dynamics of tearing modes within a slab incompressible EMHD framework, accounting for the influence of more than one non-ideal parameters such as electron inertia, resistivity and electron viscosity. Their findings emphasize the need for future research to incorporate kinetic effects and investigate EMHD tearing mode regimes, such as “electron-only” reconnection.

Zhao³⁹ incorporated the temperature in the warm EMHD model and derived the dispersion relation and investigated the electromagnetic properties of obliquely propagating whistler waves. As a future work, the warm EMHD model discussed by Zhao can be used to study linear growth rate and eigen structure of tearing and surface preserving modes change at low to moderate temperature (at high temperature, the EMHD model would break). The work on the same is underway.

IV. SUMMARY AND FUTURE SCOPE

In this study, we conducted two-dimensional PIC simulations using the OSIRIS framework to investigate the kinetic effects on tearing and surface-preserving instabilities in electron current layers, which are relevant to various space, astrophysical, and laboratory plasma environments. We started by simulating the conventional tearing instability to validate our simulation setup. After validation, we explored the kinetic effects on the tearing mode by varying the electron temperature. Our results show that the growth rate of the tearing instability initially increased with temperature, peaking around 10 eV, before declining due to the increased electron Larmor radius and consequent diffusion of magnetic fields. To support our argument, we introduced a uniform guide field, which exhibited a stabilizing effect on the tearing mode, resulting in a shift of the peak growth rate to higher temperatures.

To study the surface-preserving instability, we added a uni-

form magnetic field $C_0 = 0.06$ along the equilibrium magnetic field direction, which inhibits the tearing mode in the system. To analyze the effect of temperature on the growth rate of this mode, we ran simulations at various temperatures. The growth rate versus temperature plot shows a consistent rise, which can be attributed to the increased electron flow velocity at higher temperatures. This rise favors the instability, as it is driven by perturbations in the flow.

Finally, we also investigated the case when both the tearing and surface-preserving modes exist simultaneously in the system. Simulation runs in this scenario show that the structures (island and quadrupole) formed are asymmetric. Moreover, these structures do not remain stationary but move towards the weaker magnetic field side around the null-line. This behavior aligns with findings from studies on asymmetric magnetic reconnection. The growth rate’s temperature dependence follows a pattern similar to the pure tearing mode case, initially increasing with temperature but peaking at lower temperature value. The causes of this shift are currently being studied, considering magnetic field asymmetries and the interplay between tearing and surface-preserving modes under varying temperatures.

Future Directions:

- In our studies, we have chosen the tanh - sech profile for the equilibrium magnetic field. While this allows us to use periodic boundary conditions, the profile naturally ceases at the boundaries. Conducting studies on larger systems (using profiles with a larger extent) with appropriate boundary conditions would provide a natural comparison.
- In our studies, we have chosen $\varepsilon = 1$, which is normalized by the electron skin depth. A parametric study by choosing $\varepsilon > 1$ and $\varepsilon < 1$ needs to be carried out to understand the behavior of the two modes in these different regimes, along with the role of temperature on their behavior.
- In mixed mode cases, the magnetic field profile is asymmetric around the null line. To distinguish the effects of this asymmetry on the tearing mode and its interaction with the surface-preserving mode, a dedicated study using appropriate profiles is needed.
- Linear stability analysis using a warm EMHD (Electromagnetic Magnetohydrodynamics) model is currently underway and is essential for understanding the eigenmode structure under varying temperature conditions. This analysis will provide insights into how temperature influences the structure and stability of the modes.

ACKNOWLEDGMENTS

SM gratefully acknowledges the financial support provided by the Govt. of Gujarat under SHODH scheme. SM and GG

would like to thank Professor Abhijit Sen for useful discussions. GG would like to thank Jugal Chowdhury for providing the comments on the manuscript.

- ¹M. Yamada, R. Kulsrud, and H. Ji, “Magnetic reconnection,” *Reviews of modern physics* **82**, 603 (2010).
- ²J. B. Taylor, “Relaxation and magnetic reconnection in plasmas,” *Reviews of Modern Physics* **58**, 741 (1986).
- ³M. Yamada, “Review of controlled laboratory experiments on physics of magnetic reconnection,” *Journal of Geophysical Research: Space Physics* **104**, 14529–14541 (1999).
- ⁴R. Stenzel, M. Griskey, J. Urrutia, and K. Strohmaier, “Three-dimensional electron magnetohydrodynamic reconnection. i. fields, currents, and flows,” *Physics of Plasmas* **10**, 2780–2793 (2003).
- ⁵R. Stenzel, M. Griskey, J. Urrutia, and K. Strohmaier, “Three-dimensional electron magnetohydrodynamic reconnection. iv. instabilities, fluctuations, and emissions,” *Physics of Plasmas* **10**, 2810–2818 (2003).
- ⁶S. Bose, W. Fox, H. Ji, J. Yoo, A. Goodman, A. Alt, and M. Yamada, “Conversion of magnetic energy to plasma kinetic energy during guide field magnetic reconnection in the laboratory,” *Physical Review Letters* **132**, 205102 (2024).
- ⁷P. A. Sweet, “The neutral point theory of solar flares,” *Electromagnetic Phenomena in Cosmical Physics*, 123–134 (1958).
- ⁸E. N. Parker, “Sweet’s mechanism for merging magnetic fields in conducting fluids,” *Journal of Geophysical Research* **62**(4), 509–520 (1957).
- ⁹H. E. Petschek, “Magnetic field annihilation,” *NASA Special Publication* **50**, 425 (1964).
- ¹⁰S. Bulanov, F. Pegoraro, and A. Sakharov, “Magnetic reconnection in electron magnetohydrodynamics,” *Physics of Fluids B: Plasma Physics* **4**, 2499–2508 (1992).
- ¹¹J. Birn and E. R. Priest, *Reconnection of magnetic fields: magnetohydrodynamics and collisionless theory and observations* (Cambridge University Press, 2007).
- ¹²M. A. Shay, J. F. Drake, R. E. Denton, and D. Biskamp, “Structure of the dissipation region during collisionless magnetic reconnection,” *Journal of Geophysical Research: Space Physics* **103**, 9165–9176 (1998).
- ¹³J. Drake, M. Shay, and M. Swisdak, “The hall fields and fast magnetic reconnection,” *Physics of Plasmas* **15** (2008).
- ¹⁴D. Biskamp, “Magnetic reconnection in plasmas,” *Astrophysics and Space Science* **242**, 165–207 (1996).
- ¹⁵A. P. Matthews, “Current advance method and cyclic leapfrog for 2d multi-species hybrid plasma simulations,” *Journal of Computational Physics* **112**, 102–116 (1994).
- ¹⁶W. Daughton, V. Roytershteyn, B. Albright, H. Karimabadi, L. Yin, and K. J. Bowers, “Transition from collisional to kinetic regimes in large-scale reconnection layers,” *Physical review letters* **103**, 065004 (2009).
- ¹⁷R. Horiuchi and T. Sato, “Three-dimensional particle simulation of plasma instabilities and collisionless reconnection in a current sheet,” *Physics of Plasmas* **6**, 4565–4574 (1999).
- ¹⁸J. M. Dawson, “Particle simulation of plasmas,” *Reviews of modern physics* **55**, 403 (1983).
- ¹⁹L.-J. Chen, M. Hesse, S. Wang, D. Gershman, R. Ergun, J. Burch, N. Bessho, R. Torbert, B. Giles, J. Webster, *et al.*, “Electron diffusion region during magnetopause reconnection with an intermediate guide field: Magnetospheric multiscale observations,” *Journal of Geophysical Research: Space Physics* **122**, 5235–5246 (2017).
- ²⁰M. Hesse, M. Kuznetsova, and M. Hoshino, “The structure of the dissipation region for component reconnection: Particle simulations,” *Geophysical research letters* **29**, 4–1 (2002).
- ²¹J. Drake, M. Swisdak, K. Schoeffler, B. Rogers, and S. Kobayashi, “Formation of secondary islands during magnetic reconnection,” *Geophysical research letters* **33** (2006).
- ²²G. Gaur and P. K. Kaw, “Tearing and surface preserving electron magnetohydrodynamic modes in a current layer,” *Physics of Plasmas* **23** (2016).
- ²³V. Lukin, “Stationary nontearing inertial scale electron magnetohydrodynamic instability,” *Physics of Plasmas* **16** (2009).
- ²⁴N. Jain and J. Büchner, “Effect of guide field on three-dimensional electron shear flow instabilities in electron current sheets,” *Journal of Plasma Physics* **81**, 905810606 (2015).
- ²⁵N. Jain, J. Büchner, and P. A. Muñoz, “Nonlinear evolution of electron shear flow instabilities in the presence of an external guide magnetic field,” *Physics of Plasmas* **24** (2017).
- ²⁶R. W. Hockney and J. W. Eastwood, *Computer simulation using particles* (crc Press, 2021).
- ²⁷R. Fonseca, L. Silva, F. Tsung, V. Decyk, W. Lu, C. Ren, W. Mori, S. Deng, S. Lee, T. Katsouleas, *et al.*, “Lecture notes in computer science,” *Lecture Notes in Computer Science* **2331**, 342–351 (2002).
- ²⁸R. A. Fonseca, J. Vieira, F. Fiúza, A. Davidson, F. S. Tsung, W. B. Mori, and L. O. Silva, “Exploiting multi-scale parallelism for large scale numerical modelling of laser wakefield accelerators,” *Plasma Physics and Controlled Fusion* **55**, 124011 (2013).
- ²⁹A. Kemp, F. Fiúza, A. Debayle, T. Johzaki, W. Mori, P. Patel, Y. Sentoku, and L. Silva, “Laser–plasma interactions for fast ignition,” *Nuclear Fusion* **54**, 054002 (2014).
- ³⁰L. O. Silva, R. Fonseca, J. Tonge, J. Dawson, W. Mori, and M. Medvedev, “Interpenetrating plasma shells: near-equipartition magnetic field generation and nonthermal particle acceleration,” *The Astrophysical Journal* **596**, L121 (2003).
- ³¹R. Fonseca, T. Dalichaouch, A. Davidson, F. Cruz, F. Del Gaudio, G. Inchingolo, A. Helm, R. Lee, F. Li, J. May, *et al.*, “Osiris 4.0: A state of the art framework for kinetic plasma simulations,” in *APS Division of Plasma Physics Meeting Abstracts*, Vol. 2018 (2018) pp. PP11–023.
- ³²Presence of a guide field is known to play a stabilizing role in magnetic reconnection.
- ³³H. Cai and D. Li, “Magnetic reconnection with pressure tensor in electron magnetohydrodynamics,” *Physics of Plasmas* **16** (2009).
- ³⁴H. Cai and D. Li, “Magnetic reconnection with pressure gradient effect in compressible electron magnetohydrodynamics,” *Physics of Plasmas* **15** (2008).
- ³⁵W. Guo, D. Liu, X. Wang, and J. Wang, “Tearing mode analysis in electron magnetohydrodynamics with pressure gradient,” *AIP Advances* **10** (2020).
- ³⁶W. Guo, J. Wang, and D. Liu, “Numerical studies on electron magnetohydrodynamics tearing mode instability,” *AIP Advances* **11** (2021).
- ³⁷D. Del Sarto, F. Califano, and F. Pegoraro, “Current layer cascade in collisionless electron-magnetohydrodynamic reconnection and electron compressibility effects,” *Physics of plasmas* **12** (2005).
- ³⁸H. Betar, D. Del Sarto, A. Ghizzo, F. Brochard, and D. Zarzoso, “A numerical study of electron-magnetohydrodynamics tearing modes in parameter ranges of experimental interest,” *Physics of Plasmas* **31** (2024).
- ³⁹J. Zhao, “Properties of whistler waves in warm electron plasmas,” *The Astrophysical Journal* **850**, 13 (2017).